AD-A147 855 THEORETICAL STUDY OF LASER-INDUCED SURFACE EXCITATIONS ON A GRATING(U) ROCHESTER UNIV NY DEPT OF CHEMISTRY K T LEE ET AL. NOV 84 UROCHESTER/DC/84/TR-57 1/1

UNCLASSIFIED N00014-80-C-0472 F/G 20/5 NL

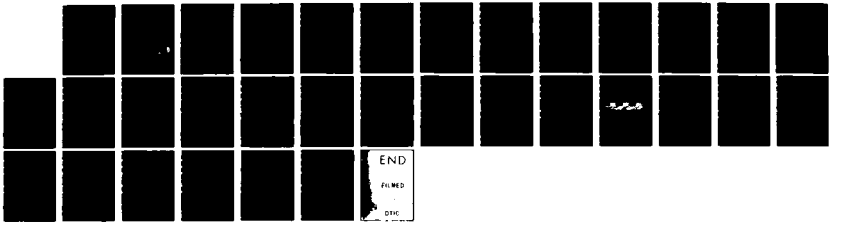

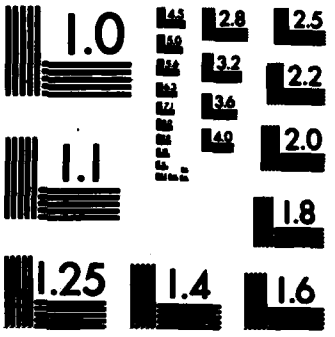

OFFICE OF NAVAL RESEARCH

Contract N00014-80-C-0472

Task No. NR 056-749

TECHNICAL REPORT No. 57

Theoretical Study of Laser-Induced Surface Excitations on a Grating

by

Ki-Tung Lee and Thomas F. George

Prepared for Publication

in

Physical Review B

Department of Chemistry
University of Rochester
Rochester, New York 14627

November 1984

4. PERFORMING ORGANIZATION REPORT NUMBER(S)		5. MONITORING ORGANIZATION REPORT NUMBER(S)
UROCHESTER/DC/84/TR-57		
6a. NAME OF PERFORMING ORGANIZATION Department of Chemistry University of Rochester	6b. OFFICE SYMBOL *(If applicable)*	7a. NAME OF MONITORING ORGANIZATION Office of Naval Research
6c. ADDRESS *(City, State and ZIP Code)* River Station Rochester, New York 14627		7b. ADDRESS *(City, State and ZIP Code)* Chemistry Program Code 472 Arlington, Virginia 22217
8a. NAME OF FUNDING/SPONSORING ORGANIZATION Office of Naval Research	8b. OFFICE SYMBOL *(If applicable)*	9. PROCUREMENT INSTRUMENT IDENTIFICATION NUMBER Contract N00014-80-C-0472
8c. ADDRESS *(City, State and ZIP Code)* Chemistry Program Code 472 Arlington, Virginia 22217		10. SOURCE OF FUNDING NOS. PROGRAM ELEMENT NO. NR 056-749 / PROJECT NO. / TASK NO. / WORK UNIT NO.

11. TITLE: Theoretical Study of Laser-Induced Surface Excitations on a Grating

12. PERSONAL AUTHOR(S): Ki-Tung Lee and Thomas F. George

13a. TYPE OF REPORT	13b. TIME COVERED	14. DATE OF REPORT *(Yr., Mo., Day)*	15. PAGE COUNT
Interim Technical	FROM _____ TO _____	November 1984	25

16. SUPPLEMENTARY NOTATION
Prepared for publication in the Physical Review B

17. COSATI CODES			18. SUBJECT TERMS *(Continue on reverse if necessary and identify by block number)*
FIELD	GROUP	SUB. GR.	GRATINGS SURFACE-EXCITATIONS LASER-INDUCED MAXWELL'S EQUATIONS ARBITRARY GRATING SHAPES NEW RESONANCE PHENOMENON

Physical Review B, in press

THEORETICAL STUDY OF LASER-INDUCED SURFACE EXCITATIONS ON A GRATING

Ki-Tung Lee and Thomas F. George

Department of Chemistry
University of Rochester
Rochester, New York 14627

Laser-induced surface excitations on a grating are studied in terms of the solutions to Maxwell's equations. A rigorous theory, derived originally for a lamellar grating, is used to study the resonance phenomenon for deep gratings. The generalization of the square-well grating to gratings of arbitrary shapes is examined numerically. A new diffraction anomaly is seen to occur when the grating depth is approximately equal to half of the wavelength of the incident laser radiation.

I. Introduction

It has been well established that impinging light on a rough metallic surface may lead to resonant excitation of surface plasma oscillations, which play an important role in interesting surface phenomena, such as surface-enhanced Raman scattering[1,2] and laser-induced periodic pattern deposition.[3] In particular, the spatial oscillation of photochemically deposited metal films is identified as the fingerprint of the oscillation of a surface plasma wave (SPW). These surface waves are related or similar to those found in Wood's anomalies[4,5] or Brewster's waves,[6] which all satisfy the same mathematical equation but with media of different electric properties. Moreover, all these waves have the same characteristics in that they propagate along the surface of a dielectric medium, with amplitudes decaying exponentially with increasing distance from the surface into the dielectrics and into the vacuum in contact with it. In the second quantization terminology, these surface waves are labelled as surface polaritons. Resonant excitation of these quasistationary modes can lead to orders of magnitude of enhancement of molecular processes occurring near or on the surface. (It has been suggested by Tsang and Kirtley[7] and later by Mill and Weber[8] that the maximum value of electric fields near gratings may be limited by grating-induced radiative damping.) Thus, a detailed understanding of the formation and the properties of these surface waves would be helpful in better understanding and controlling surface molecular rate processes and diagnosis of the properties of surfaces. (A comprehensive review of the diagnosis of surface properties can be found in Reference 9.)

A general understanding of the physical properties of these surface waves has been reviewed by Fano,[5] and recent advances in research, both theoretically and experimentally, have been reviewed by Agranovich and Mills.[10] These quasistationary modes are controlled by the following elements:

a) the wavelength of the incident radiation,

b) the angle of incidence,

c) the geometry of the surface roughness,

d) the electric properties of the surface,

e) the polarization.

One approach to the theory of surface plasma oscillations has been in terms of the collective motion of electrons in the solid.[11] It has been found, however, that the problem of resonant excitation of SPW can be treated more easily as an optical problem than as the collective motion of the electrons. In fact, both the problems of surface-enhanced Raman scattering[12] and laser-induced pattern deposition[3] have been examined by Rayleigh's perturbative diffraction theory.[13]

The formation of these evanescent waves originates a momentum transfer from the grating (roughness) to the impinging waves. Since the frequency of the impinging laser radiation is unaffected by the roughness, the modulus of the momentum of any wave must equal the one in the vacuum. Thus, momentum transfer by the roughness can only change the direction of momentum. This means that when the tangential component of the momentum of the diffractive wave,

$$k_{mt} = k_t + \frac{m}{d}, \tag{1}$$

where k_t is the tangential component of the incident wave, d is the spacing of the grating and m is an integer, is larger than the modulus of the incident momentum, k_0, then the normal component of the diffractive wave,

$$k_n = (k_0^2 - k_{mt}^2)^{1/2},$$

becomes imaginary. This corresponds to evanescent waves travelling with momentum k_{mt} along the surface and exponentially damped in the normal direction. Moreover, if the geometry is chosen so certain kinematical conditions are met, the incident photon will resonantly couple to these surface polaritons.

The effect of the grating depth on the resonant conditions has been studied recently by Garcia[14] and Neviere and Reinisch.[15] While Garcia found that the intensities of the reflectivity and the diffraction beams have their minimum at resonance, but that the reflectivity becomes a maximum for a particular value of the grating depth, Neviere and Reinisch[15] pointed out that there exists an optimum value of the grating depth for which the electromagnetic (EM) resonance contribution to the enhancement of the nonlinear optical process is the greatest, and the optimization is achieved with very shallow modulation. More recently, Glass, Weber and Mills,[16] utilizing the extinction theorem of Toigo, Marvin, Hill and Celli,[17] studied the grating-induced radiative damping of the surface polariton for grating profiles with various shapes and depths, and compared the results with those of perturbation theory. Good agreement was found for those systems investigated. All of the calculations mentioned above fall in the regime that the grating amplitude is much smaller than the incident wavelength. In this paper, we employ the square-well grating theory of Sheng, Stepleman and Sandra,[18] which is based on the formalism of a stratified medium,[19] to study a new kind of resonance condition for a grating depth comparable to the incident wavelength.

Recently, various numerical techniques[20] have been developed for the solution of diffraction problems. Although most of these are rigorous in formulation, they exhibit various degrees of effectiveness in actual calculations. Very often numerical difficulties are found either when the grating depth becomes too large[21] or when the conductivity of the grating is large.[20] The square-well grating approach[18] has been demonstrated to be numerically stable even in the regime of good conductivity and also to work well for the case of a deep grating. However, the method is restricted to a lamellar grating. We have suggested a generalization of the square-well grating theory to gratings of arbitrary shape.[22] In this paper, the numerical applicability of this generalized theory is examined. The diffraction

from gratings of arbitrary shape has attracted a lot of attention recently. Moharan and Gaylord have applied their coupled-wave theory[23] to a multilayered grating formalism,[24] while Suratteau, Cadilhac and Petit[25] formulated a "Multi-Step Lamellar Grating" (MSLG) method by extending the work of Botten and coworkers.[26] The MSLG method, which has only been applied to lossless dielectrics, is believed to be closely related to the present work. In Section II, the theory of the square-well grating and its generalization to a multilayered grating is briefly reviewed. The results and discussion are given in Section III, and a summary is presented in Section IV.

II. Theory

A. Square-Well Grating

The square-well grating formalism is based on a stratified medium model,[17] and a detailed account of the derivation can be found in a paper by Sheng et al.[16] Our main purpose in this part of Section II is to set up the notation for the generalization of the square-well grating to a multilayered grating.

Following Rayleigh's approach, the entire space is separated into three regions: the vacuum region (Region I), the dielectric region (Region III) and the corrugation region (Region II). The geometry and the coordinate system of the lamellar grating are shown in Fig. 1. In Regions I and III, the EM fields are expressed in terms of Rayleigh waves,

$$\psi^I = \exp[ik_0(\sin\theta_i x - \cos\theta_i z)] - \sum_{n=-\infty}^{\infty} R_n \exp\{ik_0[\gamma_n x + (1-\gamma_n^2)^{1/2} z]\}, \qquad (2)$$

and

$$\psi^{III} = \sum_{n=-\infty}^{\infty} T_n \exp\{ik_0[\gamma_n x - (\varepsilon-\gamma_n^2)^{1/2} z]\}. \qquad (3)$$

For p-wave scattering, ψ is the y-component of the magnetic vector, $k_0 = 2\pi/\lambda$ is the free-space wave vector of the incident laser radiation, ε is the dielectric constant of the grating, R_n and T_n are the amplitudes of the n-th reflected and transmitted diffracted orders, θ_i is the angle of incidence, and

$$\gamma_n = \sin\theta_i + n\lambda/d, \qquad (4)$$

where d is the period of the grating. (The square root with positive imaginary part will always be chosen in this paper.) The field in Region II satisfies[16]

$$\frac{\partial^2\psi^{II}}{\partial z^2} + \frac{\partial^2\psi^{II}}{\partial x^2} + \varepsilon(x)k_0^2\psi^{II} = \frac{\partial\psi^{II}}{\partial x}\frac{d}{dx}\ln[\varepsilon(x)], \tag{5}$$

where $\varepsilon(x) = \varepsilon$ for $|x - nd| \leq rd/2$, and 1 otherwise (r is a number between 0 and 1). At this stage, the problem becomes identical to that of a periodically stratified medi with a piecewise constant ε.[17] Thus, the field in Region II can be expressed in gener as

$$\psi^{II} = \sum_{\ell} X_\ell(x)[A_\ell\exp(i\Lambda_\ell z) + B_\ell\exp(-i\Lambda_\ell z)], \tag{6}$$

where Λ_ℓ^2 are the eigenvalues satisfying the transcendental equation

$$\cos(k_0 d\sin\theta_i) + \cos(\beta_\ell rd)\cos[\alpha_\ell(1-r)d] + \frac{1}{2}\left(\varepsilon\frac{\alpha_\ell}{\beta_\ell} + \frac{\beta_\ell}{\varepsilon\alpha_\ell}\right) \times \sin(\beta_\ell rd)\sin[\alpha_\ell(1-r)d] = 0, \tag{7}$$

and the associated eigenfunctions. $X_\ell(x)$ are given by

$$X_\ell(x) = \begin{cases} \cos[\beta_\ell(x+\frac{rd}{2})] + iV_0^\ell\frac{\varepsilon k_0}{\beta_\ell}\sin[\beta_\ell(x+\frac{rd}{2})], & |x| \leq \frac{rd}{2} \\ U^\ell\cos[\alpha_\ell(x-\frac{rd}{2})] + iV_1^\ell\frac{k_0}{\alpha_\ell}\sin[\alpha_\ell(x-\frac{rd}{2})], & \frac{rd}{2} \leq x \leq (1-\frac{r}{2})d \end{cases} \tag{8}$$

where $X_\ell(-rd/2)$ is normalized to 1, with

$$V_0^\ell = [\exp(ik_0 d\sin\theta_i) - M_\ell]/N_\ell, \tag{9}$$

$$V_1^\ell = \frac{i}{k_0}\frac{\beta_\ell}{\varepsilon}\sin(\beta_\ell rd) + V_0^\ell\cos(\beta_\ell rd), \tag{10}$$

$$U^\ell = \cos(\beta_\ell rd) + iV_0^\ell\frac{\varepsilon k_0}{\beta_\ell}\sin(\beta_\ell rd), \tag{11}$$

$$M_\ell = \cos(\beta_\ell rd)\cos[\alpha_\ell(1-r)d] - \frac{\beta_\ell}{\varepsilon\alpha_\ell}\sin[\alpha_\ell(1-r)d]\sin(\beta_\ell rd), \quad (12)$$

$$N_\ell = ik_0[\frac{1}{\alpha_\ell}\cos(\beta_\ell rd)\sin[\alpha_\ell(1-r)d] + \frac{\varepsilon}{\beta_\ell}\sin(\beta_\ell rd)\cos[\alpha_\ell(1-r)d], \quad (13)$$

$$\alpha_\ell = (k_0^2 - \Lambda_\ell^2)^{1/2} \quad (14)$$

$$\beta_\ell = (\varepsilon k_0^2 - \Lambda_\ell^2)^{1/2}. \quad (15)$$

The remaining task is to determine the expansion coefficients, R_n, T_n, A_ℓ and B_ℓ, by matching the analytic solutions of Maxwell's equations at the boundaries; namely, the continuity of tangential E and H fields at $z = 0$ and $z = -h$. This gives four simultaneous equations which are valid for all x:

$$\sum_n \exp(ik_0\gamma_n x_j)(\delta_{n0} - R_n) = \sum_\ell X_\ell(x_j)(A_\ell + B_\ell), \quad (16)$$

$$\sum_\ell X_\ell(x_j)[A_\ell\exp(-i\Lambda_\ell h) + B_\ell\exp(i\Lambda_\ell h)] = \sum_n \exp\{ik_0[\gamma_n x_j + (\varepsilon-\gamma_n^2)^{1/2}h]\}T_n, \quad (17)$$

$$\sum_n -ik_0[\cos\theta_i\delta_{n0} + (1-\gamma_n^2)^{1/2}R_n\exp(ik_0\gamma_n x_j)] = \sum_\ell i\frac{X_\ell}{\varepsilon}(x_j)\Lambda_\ell[A_\ell - B_\ell] \quad (18)$$

$$\sum_\ell \frac{X_\ell(x_j)}{\varepsilon} i\Lambda_\ell[A_\ell\exp(-i\Lambda_\ell h) - B_\ell\exp(i\Lambda_\ell h)] = \frac{1}{\varepsilon}\sum_n -ik_0(\varepsilon-\gamma_n^2)^{1/2}T_n\exp\{ik_0\gamma_n x_j + (\varepsilon-\gamma_n^2)^{1/2}h\}. \quad (19)$$

Employing the point matching method, we can rewrite Eqs. (16) - (19) in matrix notation as

$$(\underset{\sim}{D} - \underset{\sim}{R}) = \underset{\approx}{\Gamma}^{-1}\underset{\approx}{X}(\underset{\sim}{A} + \underset{\sim}{B}), \quad (20)$$

$$\underset{\approx}{\Gamma}^{-1}\,\underset{\approx}{X}(\underset{\approx}{\Sigma}\,\underset{\sim}{A} + \underset{\approx}{\Sigma}^{-1}\underset{\sim}{B}) = \underset{\approx}{\Delta}\underset{\sim}{T}, \tag{21}$$

$$-\underset{\approx}{\Pi}(\underset{\sim}{R}+\underset{\sim}{D}) = \underset{\approx}{\Gamma}^{-1}\underset{\approx}{\Omega}(\underset{\sim}{A}-\underset{\sim}{B}), \tag{22}$$

$$\underset{\approx}{\Gamma}^{-1}\,\underset{\approx}{\Omega}(\underset{\approx}{\Sigma}\,\underset{\sim}{A} - \underset{\approx}{\Sigma}^{-1}\underset{\sim}{B}) = -\underset{\approx}{\xi}\,\underset{\approx}{\Delta}\underset{\sim}{T}, \tag{23}$$

where

$$P_{jn} = \exp(ik_0\gamma_n x_j), \tag{24}$$

$$X_{j\ell} = X_\ell(x_j), \tag{25}$$

$$\Omega_{j\ell} = \frac{\Lambda_\ell}{\epsilon}\,X_\ell(x_j), \tag{26}$$

$$\Sigma_{j\ell} = \exp(-i\Lambda_\ell h)\delta_{j\ell}, \tag{27}$$

$$\Pi_{nj} = k_0(1-\gamma_n^2)^{1/2}\delta_{nj}, \tag{28}$$

$$\Delta_{nj} = \exp[ik_0(\epsilon-\gamma_n^2)^{1/2}h]\delta_{nj}, \tag{29}$$

$$\xi_{nj} = \frac{k_0}{\epsilon}\,(\epsilon-\gamma_n^2)^{1/2}\delta_{nj}. \tag{30}$$

D is defined as $D_m = \delta_{m0}$. After some manipulation, we have the expressions for R and T in matrix form as

$$\underset{\sim}{R} = (\underset{\approx}{\Theta}-\underset{\approx}{\Pi})^{-1}(\underset{\approx}{\Theta}+\underset{\approx}{\Pi})\underset{\sim}{D} \tag{31}$$

with

$$\underset{\approx}{\Theta} = -\{[\underset{\approx}{\Gamma}^{-1}\underset{\approx}{\Omega}+\underset{\approx}{\xi}\underset{\approx}{\Gamma}^{-1}\underset{\approx}{X}]\underset{\approx}{\Sigma} + (\underset{\approx}{\Gamma}^{-1}\underset{\approx}{\Omega}-\underset{\approx}{\xi}\underset{\approx}{\Gamma}^{-1}\underset{\approx}{X})\underset{\approx}{\Sigma}^{-1}]\underset{\approx}{\Omega}^{-1}\underset{\approx}{\Gamma}\}^{-1}$$

$$\times\,[(\underset{\approx}{\Gamma}^{-1}\underset{\approx}{\Omega}+\underset{\approx}{\xi}\underset{\approx}{\Gamma}^{-1}\underset{\approx}{X})\underset{\approx}{\Sigma} - (\underset{\approx}{\Gamma}^{-1}\underset{\approx}{\Omega}-\underset{\approx}{\xi}\underset{\approx}{\Gamma}^{-1}\underset{\approx}{X})\underset{\approx}{\Sigma}^{-1}]\underset{\approx}{X}^{-1}\underset{\approx}{\Gamma} \tag{32}$$

and

$$\underset{\sim}{T} = 2\underset{\approx}{\Delta}^{-1}\underset{\approx}{K}^{-1}\underset{\approx}{X}^{-1}\underset{\approx}{\Gamma}(\underset{\sim}{D} - \underset{\sim}{R}), \tag{33}$$

where

$$\underset{\approx}{K} = \underset{\approx}{\Sigma}^{-1}(\underset{\approx}{X}^{-1}\underset{\approx}{\Gamma} - \underset{\approx}{\Omega}^{-1}\underset{\approx\approx}{\Gamma\xi}) + \underset{\approx}{\Sigma}(\underset{\approx}{X}^{-1}\underset{\approx}{\Gamma} + \underset{\approx}{\Omega}^{-1}\underset{\approx\approx}{\Gamma\xi}). \tag{34}$$

For $h = 0$, both $\underset{\approx}{\Sigma}$ and $\underset{\approx}{\Delta}$ reduce to identity matrices. In this case, $\underset{\approx}{\Theta}$ becomes $-\underset{\approx}{\xi}$, which directly implies

$$\underset{\sim}{R} = (\underset{\approx}{\xi}+\underset{\approx}{\Pi})^{-1}(\underset{\approx}{\xi}-\underset{\approx}{\Pi})\underset{\sim}{D} \tag{35}$$

and

$$\underset{\sim}{T} = \underset{\sim}{D} - \underset{\sim}{R}, \tag{36}$$

which are the correct expressions for flat surfaces. In the case of a very deep grating, $h \to \infty$, and for Λ_ℓ with an imaginary part of any size, $\Sigma_{\ell\ell} \to \infty$, then $\underset{\approx}{\Theta}$ can be reduced to a simple form, $-\underset{\approx\approx}{\Omega X}^{-1}$, and the partial field $\underset{\sim}{\Delta T}$ goes to zero. The resonant excitation conditions are given mathematically by the zero's of the expression $(\underset{\approx}{\Theta}+\underset{\approx}{\Pi})^{-1}(\underset{\approx}{\Theta}-\underset{\approx}{\Pi})$ and physically are governed by the five parameters given in Section I. Although these parameters have different degrees of importance in the control of the resonant excitation of the surface plasma oscillations, one can, with appropriate choice of these five parameters, engineer some interesting surface phenomena. Here, we focus on how the depth of the square-well grating may introduce such phenomena.

B. Multilayered Grating

We now extend the square-well grating formalism to a multilayered grating theory which can model gratings of arbitrary shape. This involves the extension of the concept of a periodic stratified medium to a two-dimensional scheme. A schematic diagram of the multilayered grating is illustrated in Fig. 2, where

Region II is divided into subregions. In each subregion, the electromagnetic field is expressed as in Eq.(6),

$$\psi_m^{II} = \sum_\ell X_\ell^m(x)[A_\ell^m \exp(i\Lambda_\ell^m z) + B_\ell^m \exp(-i\Lambda_\ell^m z)], \tag{37}$$

where m is the layer index. The characteristic equation of each layer is the same as Eq. (7). However, layers differ from each other by different values of r, which is a measure of the amount of metal within a grating period. Following the methodology of the square-well grating, we match the fields at the boundaries of each region and subregion. Hence, we have

$$\underset{\approx}{\Gamma}^{-1}\underset{\approx}{X}_0(\underset{\sim}{A}_0 + \underset{\sim}{B}_0) = \underset{\sim}{D} - \underset{\sim}{R}, \tag{38}$$

$$\underset{\approx}{\Gamma}^{-1}\underset{\approx}{X}_n(\underset{\approx}{\Sigma}_{n,n+1}\underset{\sim}{A}_n + \underset{\approx}{\Sigma}_{n,n+1}^{-1}\underset{\sim}{B}_n) = \underset{\approx\sim}{\Delta T}, \tag{39}$$

$$\underset{\approx}{\Gamma}^{-1}\underset{\approx}{\Omega}_0(\underset{\sim}{A}_0 - \underset{\sim}{B}_0) = -\underset{\approx}{\Pi}(\underset{\sim}{D} + \underset{\sim}{R}), \tag{40}$$

$$\underset{\approx}{\Gamma}^{-1}\underset{\approx}{\Omega}_n(\underset{\approx}{\Sigma}_{n,n+1}\underset{\sim}{A}_n - \underset{\approx}{\Sigma}_{n,n+1}^{-1}\underset{\sim}{B}_n) = -\underset{\approx\approx\sim}{\xi\Delta T} \tag{41}$$

$$\underset{\approx}{X}_{m-1}(\underset{\approx}{\Sigma}_{m-1,m}\underset{\sim}{A}_{m-1} + \underset{\approx}{\Sigma}_{m-1,m}^{-1}\underset{\sim}{B}_{m-1}) = \underset{\approx}{X}_{m+1}(\underset{\approx}{\Sigma}_{m,m}\underset{\sim}{A}_m + \underset{\approx}{\Sigma}_{m,m}^{-1}\underset{\sim}{B}_m) \tag{42}$$

$$\underset{\approx}{\Omega}_{m-1}(\underset{\approx}{\Sigma}_{m-1,m}\underset{\sim}{A}_{m-1} - \underset{\approx}{\Sigma}_{m-1,m}^{-1}\underset{\sim}{B}_{m-1}) = \underset{\approx}{\Omega}_{m+1}(\underset{\approx}{\Sigma}_{m,m}\underset{\sim}{A}_m - \underset{\approx}{\Sigma}_{m,m}^{-1}\underset{\sim}{B}_m), \tag{43}$$

with m = 1, ... n, and the grating has n+1 layers with a thickness of h. The elements of the Σ matrix are given as

$$(\underset{\approx}{\Sigma}_{u,v})_{p,q} = \exp(-i\Lambda_p^u v\, h)\, \delta_{pq}. \tag{44}$$

All other matrices are defined as in Part A but with a subregion index. It is trivial to generalize the formalism to treat a different thickness for each layer. For simplicity, we choose each layer to have the same thickness.

In order to find expressions for $\underset{\sim}{R}$ and $\underset{\sim}{T}$, we construct the two supermatrix equations,

$$\left(\begin{array}{c|c} \Gamma^{-1}X_0 & \Gamma^{-1}X_0 \\ \hline \Gamma^{-1}\Omega_0 & -\Gamma^{-1}\Omega_0 \end{array}\right)\begin{pmatrix} A_0 \\ B_0 \end{pmatrix} = \begin{pmatrix} D-R \\ -\Pi(D+R) \end{pmatrix} \tag{45}$$

and

$$\left(\begin{array}{c|c} \Gamma^{-1}X_n\Sigma_{n,n+1} & \Gamma^{-1}X_n\Sigma^{-1}_{n,n+1} \\ \hline \Gamma^{-1}\Omega_n\Sigma_{n,n+1} & -\Gamma^{-1}\Omega_n\Sigma^{-1}_{n,n+1} \end{array}\right)\begin{pmatrix} A_n \\ B_n \end{pmatrix} = \begin{pmatrix} \Delta T \\ -\xi\Delta T \end{pmatrix}, \tag{46}$$

where for simplicity we have dropped the matrix notation. We notice that the A's and B's are related by the recursive relationship

$$\left(\begin{array}{c|c} \Sigma_{n,n} & \Sigma^{-1}_{n,n} \\ \hline \Sigma_{n,n} & -\Sigma^{-1}_{n,n} \end{array}\right)\begin{pmatrix} A_n \\ B_n \end{pmatrix} = \left(\begin{array}{c|c} X_n^{-1}X_{n-1}\Sigma_{n-1,n} & X_n^{-1}X_{n-1}\Sigma^{-1}_{n-1,n} \\ \hline \Omega_n^{-1}\Omega_{n-1}\Sigma_{n-1,n} & -\Omega_n^{-1}\Omega_{n-1}\Sigma^{-1}_{n-1,n} \end{array}\right)\begin{pmatrix} A_{n-1} \\ B_{n-1} \end{pmatrix}. \tag{47}$$

Hence, we have

$$\begin{pmatrix} A_n \\ B_n \end{pmatrix} = \begin{pmatrix} a & b \\ c & d \end{pmatrix}\begin{pmatrix} A_0 \\ B_0 \end{pmatrix}, \tag{48}$$

where

$$\begin{aligned}\begin{pmatrix} a & b \\ c & d \end{pmatrix} = \frac{(-1)^n}{2^n} &\left(\begin{array}{c|c} \Sigma^{-1}_{nn} & \Sigma^{-1}_{nn} \\ \hline \Sigma_{nn} & -\Sigma_{nn} \end{array}\right)\left(\begin{array}{c|c} X_n^{-1}X_{n-1}\Sigma_{n-1,n} & X_n^{-1}X_{n-1}\Sigma^{-1}_{n-1,n} \\ \hline \Omega_n^{-1}\Omega_{n-1}\Sigma_{n-1,n} & -\Omega_n^{-1}\Omega_n\Sigma^{-1}_{n-1,n} \end{array}\right) \\ &\times \left(\begin{array}{c|c} \Sigma^{-1}_{n-1,n-1} & \Sigma^{-1}_{n-1,n-1} \\ \hline \Sigma_{n-1,n-1} & -\Sigma_{n-1,n-1} \end{array}\right)\left(\begin{array}{c|c} X_{n-1}^{-1}X_{n-2}\Sigma_{n-2,n-1} & X_{n-1}^{-1}X_{n-2}\Sigma_{n-2,n-1} \\ \hline \Omega_{n-1}^{-1}\Omega_{n-2}\Sigma_{n-2,n-1} & -\Omega_{n-1}^{-1}\Omega_{n-2}\Sigma_{n-2,n-1} \end{array}\right) \\ &\times \cdots \times \left(\begin{array}{c|c} X_1^{-1}X_0\Sigma_{0,1} & X_1^{-1}X_0\Sigma^{-1}_{0,1} \\ \hline \Omega_1^{-1}\Omega_0\Sigma_{0,1} & -\Omega_1\,\Omega_0\Sigma^{-1}_{0,1} \end{array}\right).\end{aligned} \tag{49}$$

Substituting Eqs. (46) and (48) into (45), we have

$$\begin{pmatrix} K & L \\ M & N \end{pmatrix} \begin{pmatrix} D-R \\ -\Pi(D+R) \end{pmatrix} = \begin{pmatrix} \Delta T \\ -\xi\Delta T \end{pmatrix}, \tag{50}$$

where

$$\begin{pmatrix} K & L \\ M & N \end{pmatrix} = \frac{1}{2}\left(\begin{array}{c|c} \Gamma^{-1}\chi_n\Sigma_{n,n+1} & \Gamma^{-1}\chi_n\Sigma_{n,n+1}^{-1} \\ \hline \Gamma^{-1}\Omega_n\Sigma_{n,n+1} & -\Gamma^{-1}\Omega_n\Sigma_{n,n+1}^{-1} \end{array}\right)$$

$$\times \begin{pmatrix} a & b \\ c & d \end{pmatrix} \left(\begin{array}{c|c} \chi_0^{-1}\Gamma & \Omega_0^{-1}\Gamma \\ \hline \chi_0^{-1}\Gamma & -\Omega_0^{-1}\Gamma \end{array}\right). \tag{51}$$

The expressions for R and T are then given as

$$R = \{(\xi K + M) + (\xi L + N)\Pi)\}^{-1}\{(\xi K + M) - (\xi L + N)\Pi\}D \tag{52}$$

and

$$T = \Delta^{-1}(L^{-1} + N^{-1}\xi)^{-1}(L^{-1}K - N^{-1}M)(D - R). \tag{53}$$

Equations (52) and (53) are now all we require to calculate the fields at the peaks and troughs of the grating.

III. Results and Discussion

A. Square-Well Grating

Numerical calculations have been carried out for a diffraction system with an incident wavelength of $\lambda = 6471$ Å, a grating periodicity of $d = 1$ μm, and the incident angle fixed perpendicular to the grating surface. Under this configuration, the (first-order) perturbation theory predicts no resonant excitation. The diffraction amplitudes are computed as a function of the groove depth for a silver grating with the dielectric constant, $\varepsilon = -17.42 + 0.58i$, chosen to fit experimental data.[18] Results are plotted in Fig. 3 for the three lowest diffraction orders. Since the

angle of emergence for R_2 is complex, R_2 is a surface wave. As shown in Fig. 3, for a ratio of the grating amplitude to the period of 0.283, the reflected beam is at its minimum, while the first- and second-order diffraction beams are at their maxima.

To understand this behavior, one can draw an analogy to resonant scattering theory, in particular, the bound-continuum interaction problem,[27] where a quasibound state plays the role as a coupling between the bound state and the continuum states. At the resonant energy, an interference structure, which is due to a competition between two equally possible pathways, occurs in the cross section. In the present case, the grating roughness serves as the coupling between the incident wave and the surface waves. At an optimum depth, the incident wave couples strongly with the surface waves. Thus, the resonance occurs. Moreover, the direct and indirect diffraction channels interfere each other and construct the Fano-type interference structure in the first-order diffraction beam. The resonance arises when the cavity (the groove) has a depth of approximately half of the incident wavelength, which is analogous to the case of acoustic resonances in an open-ended organ pipe occurring when $(n+\frac{1}{2})\lambda$ equals the length of the pipe, where n is an integer. In the present case, we believe that the deviation from precisely a half is partially due to the fact that the delectric constant of the Ag grating has a finite nonzero imaginary part, such that the damping mechanism leads to a width as well as a shift in the resonant condition.[28] A calculation similar to the one of Glass, Weber and Mill[16] would be helpful to further understand these frequency shifts and damping rates, which is being carried out in our laboratory. As far as we know, this Fano-type interference resonance phenomenon by diffraction from a grating has never been reported before.

B. Layered Grating

In this part, we discuss the numerical applicability of the formalism derived in Part B of Section II. We test the formalism by separating the square-well grating into a fictitious layered grating, as shown in Fig. 4. We then apply the multilayered grating formalism to this fictitious layered grating for four and ten

layers. Numerical results are compared with those of the square-well grating in Table I for the first three orders of diffraction beams at various grating depth. First, the results for four layers are almost identical with those for ten layers. This implies that the method is stable for a multilayered configuration, which is important for modeling gratings of different shapes. Second, the layered grating results are, in general, in good agreement with the square-well grating results, except near resonance, especially when the numbers are small. We believe this discrepancy is due to the degree of accuracy of the matrix inversion, since in the layered grating formalism one needs to invert matrices which are twice the size of those in the square-well grating approach. These matrices appear to become singular whenever the scattering is at resonance. Moreover, we find that the expression for T_n, Eq. (53), is unstable, especially when the grating amplitude is large. This also occurs in the square-well case when T_n takes the form of Eq. (53). A more stable expression might be achieved by first evaluating the A and B coefficients.

We now turn to a calculation on a three-layered grating. The surface profile has a structure somewhat between a sawtooth grating and a sinusoidal grating, as shown in Fig. 2c. We have calculated the average field at the peak and at the trough of the grating as a function of the grating depth, with the same scattering parameters as above and with values of r (see Fig. 1) as 0.1, 0.3 and 0.5. The results are presented in Table II. We find that T_n begins to exhibit unstable behavior as the ratio of the grating amplitude to the period reaches 0.2. Otherwise, both fields are convergent and stable.

The difficulties in this layered grating approach arise from the evaluation of the nonlinear eigenvalues of Eq. (7). As mentioned by Sheng et al,[18] eigenfunctions whose eigenvalues form complex conjugate pairs should not be separated. While truncation of the matrices is inevitable and the number of eigenfunctions used for each layer should be equal, a tremendous amount of manual labor and computer time are required to match these two criteria. This is a potential problem in modelling a realistic profile.

IV. Summary

A new diffraction anomaly is seen to occur when the grating amplitude is approximately equal to half of the incident wavelength. When the resonance condition is met, the radiated energy (the scattered light) changes its "preferred" direction, and at the same time surface waves are excited.

A new multilayered grating method has been formulated to model grating profiles of arbitrary shape. The field at the peak remains stable as the grating depth increases, while the field at the trough (inside the metal) does not. Difficulties are found in choosing an optimum basis set. A supercomputer would be helpful for applying this multilayered grating formalism to model specific surface profiles.

Acknowledgments

This research was supported by the Office of Naval Research and the Air Force of Scientific Research (AFSC), United States Air Force, under Grant AFOSR-82-0046. The United States Government is authorized to reproduce and distribute reprints for governmental purposes notwithstanding any copyright notation hereon. TFG acknowledges the Camille and Henry Dreyfus Foundation for a Teacher-Scholar Award (1975-84). We acknowledge helpful conversations with Michael Hutchinson and K. C. Liu.

References

1. E. Burstein, C. Y. Chen and S. Lundqvist, in Light Scattering in Solids, ed. by J. L. Birman, H. Z. Cummins and K. K. Rebane (Plenum, New York, 1979), p. 479 ff.

2. For a comprehensive review, see R. K. Chang and T. E. Furtak, Eds., Surface-Enhanced Raman Scattering (Plenum, New York, 1981).

3. S. R. J. Brueck and D. J. Ehrlich, Phys. Rev. Lett. 48, 1678 (1982).

4. R. W. Wood, Phil. Mag. 4, 393 (1902); 23, 310 (1912); Phys. Rev. 48, 928 (1935).

5. U. Fano, J. Opt. Soc. Am. 31, 213 (1941).

6. a) M. C. Hutley and D. Maystre, Opt. Commun. 19, 431 (1976).
   b) D. Maystre and R. Petit, Opt. Commun. 17, 196 (1976).

7. J. C. Tsang, J. R. Kirtley and T. N. Theis, Solid State Commun. 35, 667 (1980).

8. D. L. Mills and M. Weber, Phys. Rev. B 26, 1075 (1982).

9. For example, see F. R. Aussanegg, A. Leitner and M. E. Lippitsch, Eds., Surfaces Studies with Lasers (Springer-Verlag, New York, 1983).

10. A. A. Maradudin, in Surface Polaritons, ed. by V. M. Agranovich and D. L. Mills, (North-Holland, New York, 1982), p. 405 ff.

11. R. H. Ritchie, Surf. Sci. 34, 1 (1973), and references cited therein.

12. S. S. Jha, J. R. Kirtley and J. C. Tsang, Phys. Rev. B 22, 3973 (1980).

13. Lord Rayleigh, Proc. R. Soc. London, Ser. A, 79, 399 (1907).

14. N. Garcia, Opt. Commun. 45, 307 (1983).

15. M. Neviere and R. Reinsch, Phys. Rev. B 10, 5403.

16. N. E. Glass, M. Weber and D. L. Mills, Phys. Rev. B 29, 6548 (1984).

17. F. Toigo, A. Marvin, C. Celli and N. R. Hill, Phys. Rev. B 15, 5618 (1977).

18. P. Sheng, R. S. Stepleman and P. N. Sandia, Phys. Rev. B 26, 2907 (1982).

19. M. Born and E. Wolf, Principles of Optics, 6th Ed. (Pergamon, New York, 1983), pp. 51-70.

20. For example, see R. Petit, Ed., Electromagnetic Theory of Diffraction Gratings (Springer, New York, 1980).

21. N. Garcia, V. Celli and N. R. Hill, Phys. Rev. B 18, 5184 (1978).

22. M. Hutchinson, K. T. Lee, W. C. Murphy, A. C. Beri and T. F. George, in Laser-Controlled Chemical Processing of Surfaces, ed. by A. W. Johnson and D. J. Ehrlich (Elsevier, New York, 1984), in press.

23. M. G. Moharan and T. K. Gaylord, J. Opt. Soc. Am. 71, 811 (1981).

24. M. G. Moharan and T. K. Gaylord, J. Opt. Soc. Am. 72, 1385 (1982).

25. J. Y. Suratteau, M. Cadilhac and R. Petit, J. Optics (Paris) 14, 273 (1983).

26. L. C. Botten, M. S. Craig, R. C. McPhedran, J. L. Adams and J. R. Andrewartha, Opt. Acta 28, 413 (1981); 28, 1087 (1981).

27. U. Fano, Phys. Rev. 124, 1866 (1961).

28. J. D. Jackson, Classical Electrodynamics, 2nd Ed. (Wiley, New York, 1975), p. 356.

Table I

The diffraction amplitudes of the first three orders for different numbers of layers in the square-well grating and for different ratios of the amplitude to the period.

		# layers		
	h/d	1	4	10
$\|R_0\|$	.10	.9712	.9739	.9739
	.20	.9551	.9588	.9588
	.28	.2367	.1969	.1969
$\|R_1\|$	.10	.1744	.1567	.1567
	.20	.2298	.2110	.2110
	.28	.8551	.8478	.8478
$\|R_2\|$	.10	.0251	.0310	.0310
	.20	.0411	.0430	.0430
	.28	.2775	.2055	.2054

Table II

The average field intensity at the peak and at the trough, as a function of the ratio of the grating amplitude to the period, for a three-layered grating with a profile as described in Fig. 2c.

h/d	$\|\bar{\Psi}\|^2$ peak	$\|\bar{\Psi}\|^2$ trough
.003	1.020	.137
.006	1.057	.923(-1)
.009	1.089	.646(-1)
.012	1.117	.469(-1)
.015	1.114	.352(-1)
.018	1.168	.270(-1)
.021	1.191	.212(-1)
.024	1.211	.170(-1)
.027	1.230	.139(-1)
.030	1.248	.115(-1)
.060	1.363	.288(-2)
.090	1.419	.112(-2)
.120	1.452	.515(-2)
.150	1.473	.250(-3)
.180	1.491	.120(-3)

Figure Captions

1. Geometry and coordinate system for a p-wave incident on a square-well grating.

2. (a) Sinusoidal grating. The hatched area represents the metal.
   (b) Square-well grating showing a separation into three layers, one of which is periodic in the x-direction and two of which are uniform.
   (c) Generalization of the square-well grating in which there are three periodic layers.

3. (a) The magnitudes of the zeroth- and second-order diffraction amplitudes plotted as a function of the ratio of the amplitude to the period (d = 1000 nm).

   (b) The magnitude of the first-order amplitude plotted as a function of the ratio of the amplitude to the period (d = 1000 nm), with r = 0.5 .

4. Schematic diagram for a fictitious square-well layered grating.

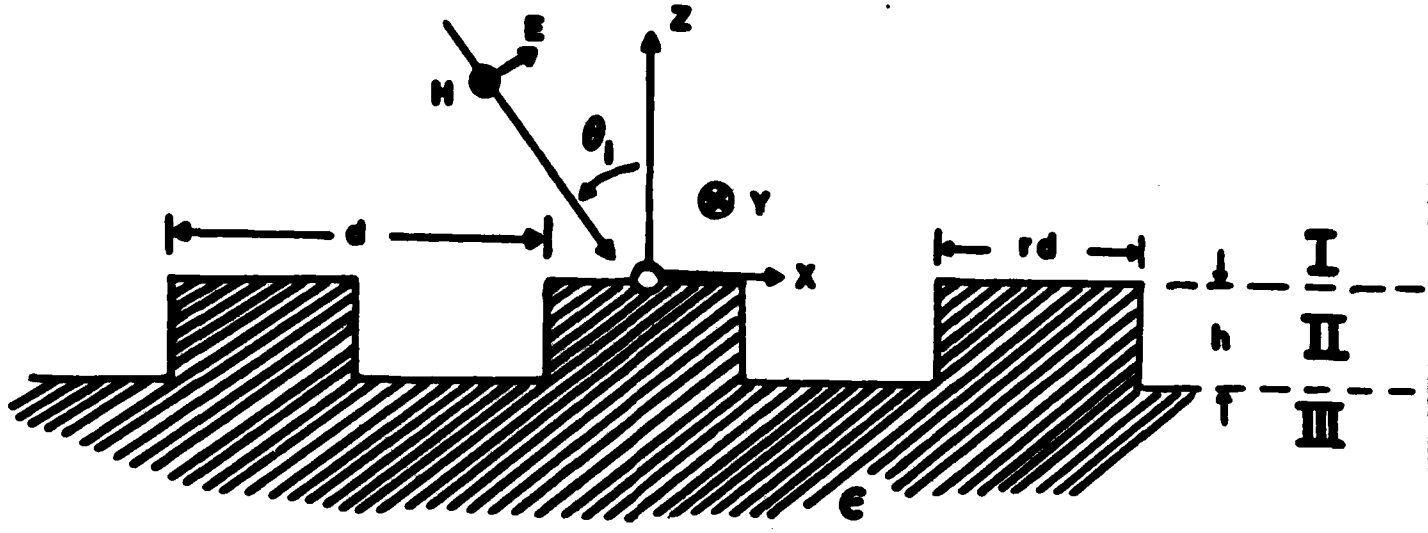
E
H
Z
θ_i
Y
X
d
rd
I
h
II
III
ϵ

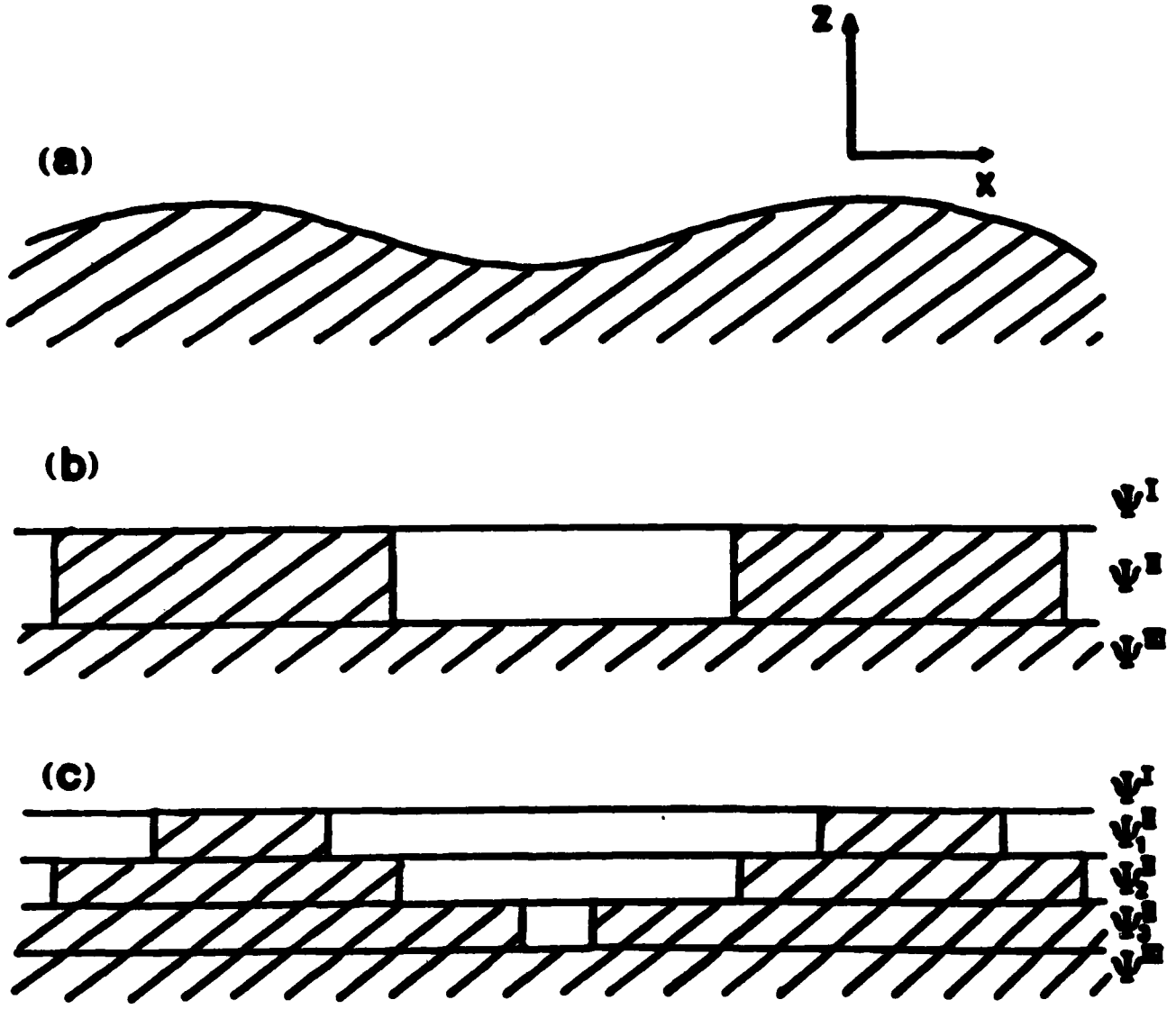
z
x
(a)
(b)
Ψ^{I}
Ψ^{II}
Ψ^{III}
(c)
Ψ^{I}

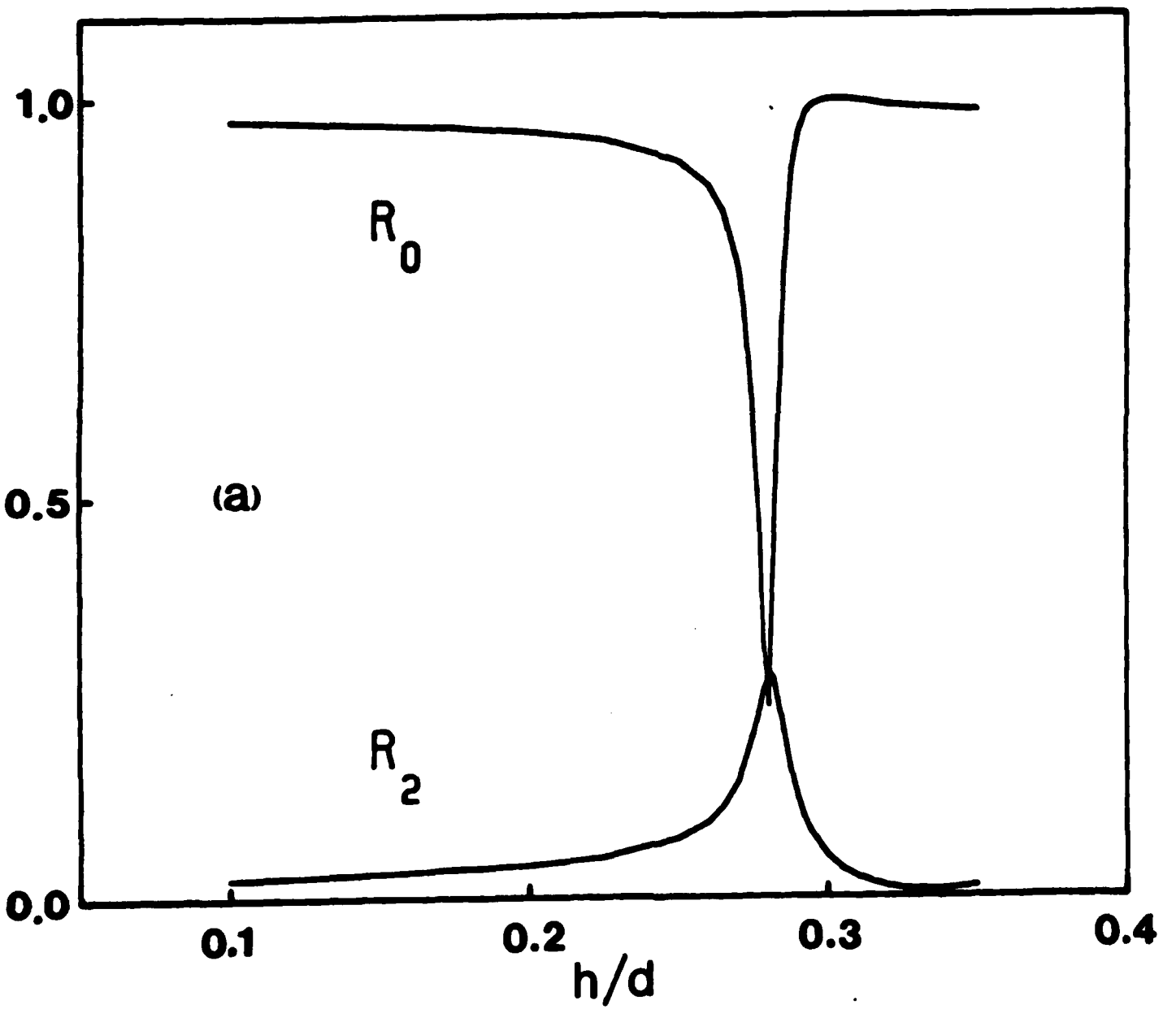
1.0
0.5
0.0
(a)
R_0
R_2
0.1
0.2
0.3
0.4
h/d

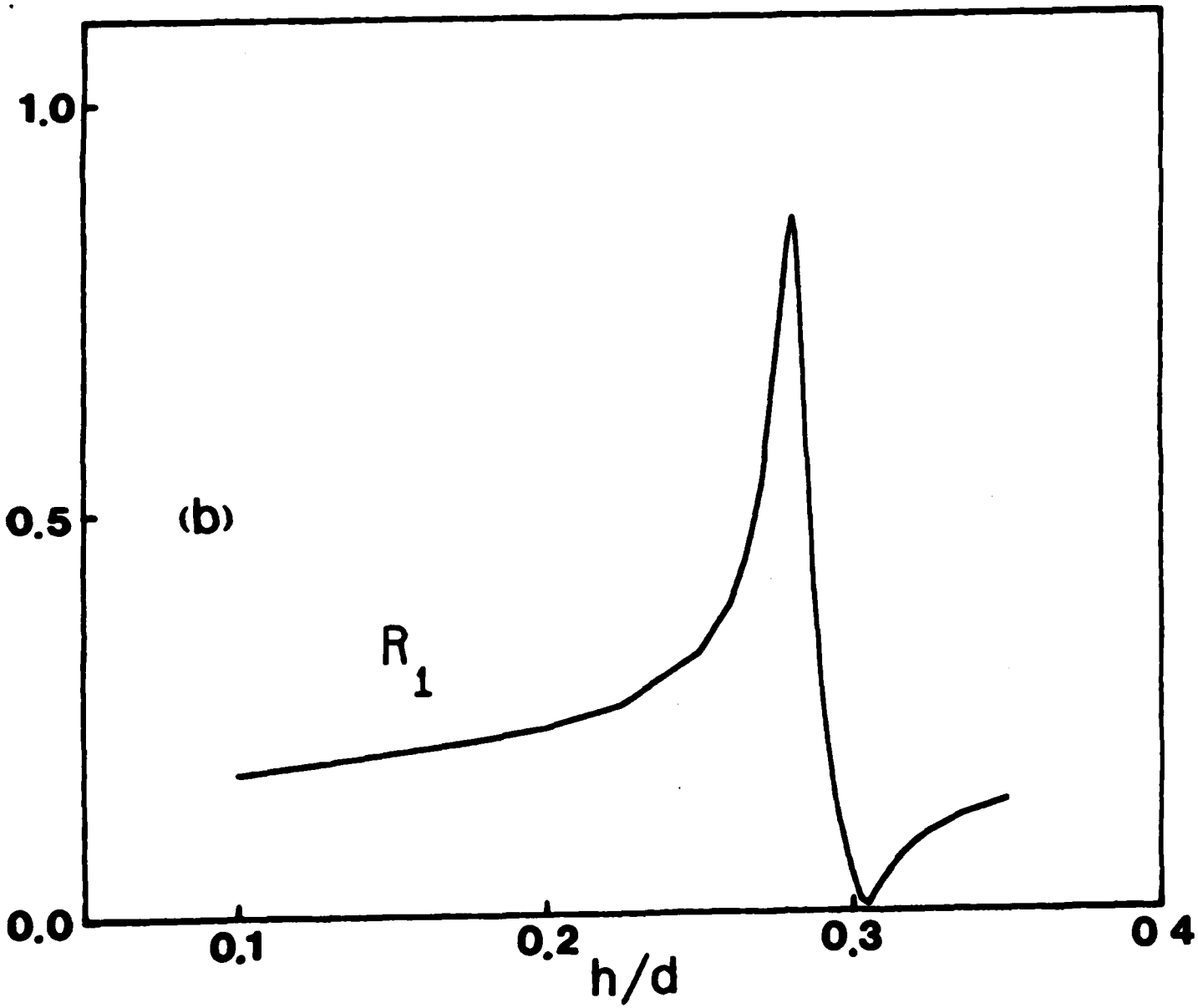
1.0
0.5
0.0
(b)
R_1
0.1
0.2
0.3
0 4
h/d

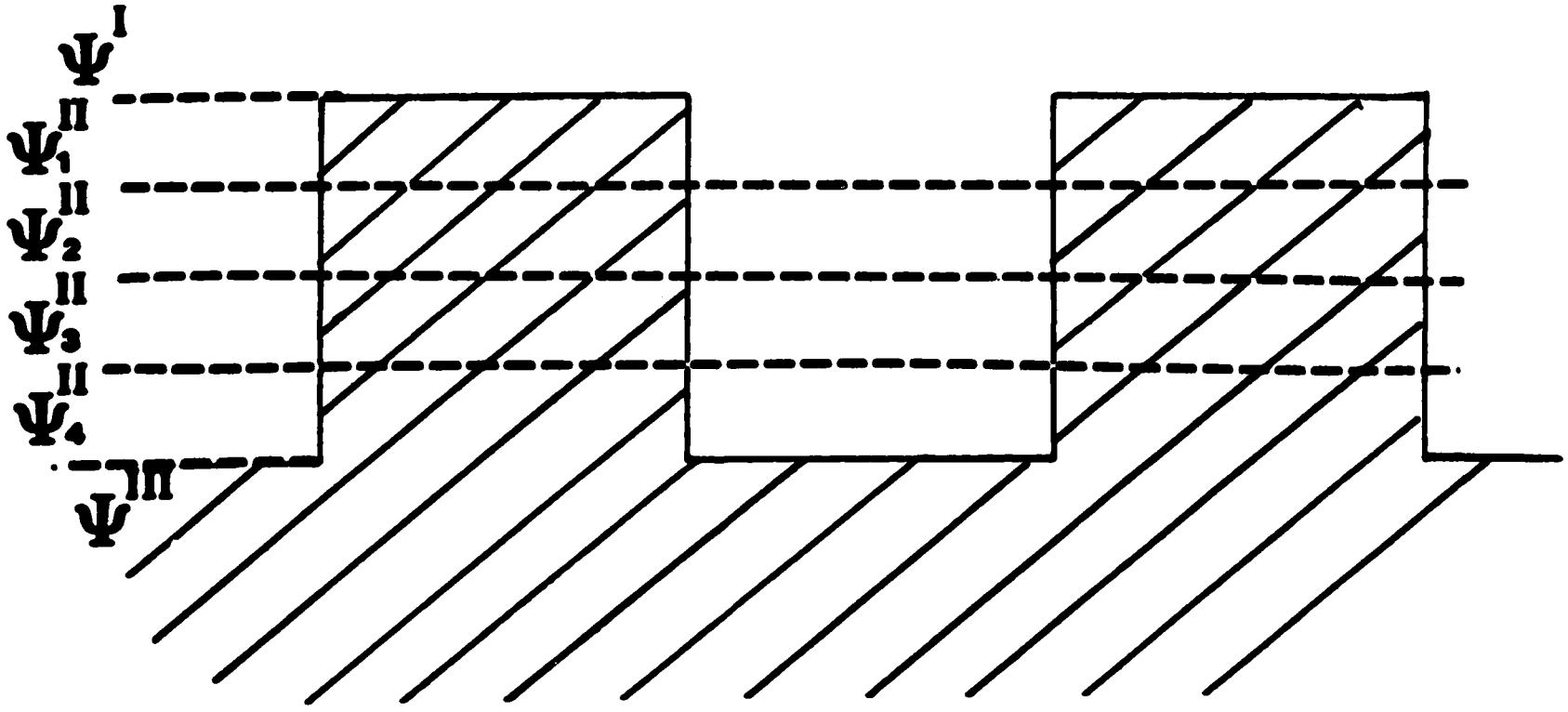
Ψ^{I}
Ψ_1^{II}
Ψ_2^{II}
Ψ_3^{II}
Ψ_4^{II}
Ψ^{III}

DL/413/83/01
GEN/413-2

TECHNICAL REPORT DISTRIBUTION LIST, GEN

	No. Copies
Office of Naval Research Attn: Code 413 800 N. Quincy Street Arlington, Virginia 22217	2
Dr. Bernard Douda Naval Weapons Support Center Code 5042 Crane, Indiana 47522	1
Commander, Naval Air Systems Command Attn: Code 310C (H. Rosenwasser) Washington, D.C. 20360	1
Naval Civil Engineering Laboratory Attn: Dr. R. W. Drisko Port Hueneme, California 93401	1
Defense Technical Information Center Building 5, Cameron Station Alexandria, Virginia 22314	12
DTNSRDC Attn: Dr. G. Bosmajian Applied Chemistry Division Annapolis, Maryland 21401	1
Dr. William Tolles Superintendent Chemistry Division, Code 6100 Naval Research Laboratory Washington, D.C. 20375	1
Dr. David Young Code 334 NORDA NSTL, Mississippi 39529	1
Naval Weapons Center Attn: Dr. A. B. Amster Chemistry Division China Lake, California 93555	1
Scientific Advisor Commandant of the Marine Corps Code RD-1 Washington, D.C. 20380	1
U.S. Army Research Office Attn: CRD-AA-IP P.O. Box 12211 Research Triangle Park, NC 27709	1
Mr. John Boyle Materials Branch Naval Ship Engineering Center Philadelphia, Pennsylvania 19112	1
Naval Ocean Systems Center Attn: Dr. S. Yamamoto Marine Sciences Division San Diego, California 91232	1
Dr. David L. Nelson Chemistry Division Office of Naval Research 800 North Quincy Street Arlington, Virginia 22217	1

DL/413/83/01
056/413-2

ABSTRACTS DISTRIBUTION LIST, 056/625/629

Dr. G. A. Somorjai
Department of Chemistry
University of California
Berkeley, California 94720

Dr. J. Murday
Naval Research Laboratory
Surface Chemistry Division (6170)
455 Overlook Avenue, S.W.
Washington, D.C. 20375

Dr. J. B. Hudson
Materials Division
Rensselaer Polytechnic Institute
Troy, New York 12181

Dr. Theodore E. Madey
Surface Chemistry Section
Department of Commerce
National Bureau of Standards
Washington, D.C. 20234

Dr. J. E. Demuth
IBM Corporation
Thomas J. Watson Research Center
P.O. Box 218
Yorktown Heights, New York 10598

Dr. M. G. Lagally
Department of Metallurgical
and Mining Engineering
University of Wisconsin
Madison, Wisconsin 53706

Dr. R. P. Van Duyne
Chemistry Department
Northwestern University
Evanston, Illinois 60637

Dr. J. M. White
Department of Chemistry
University of Texas
Austin, Texas 78712

Dr. D. E. Harrison
Department of Physics
Naval Postgraduate School
Monterey, California 93940

Dr. W. Kohn
Department of Physics
University of California, San Diego
La Jolla, California 92037

Dr. R. L. Park
Director, Center of Materials
Research
University of Maryland
College Park, Maryland 20742

Dr. W. T. Peria
Electrical Engineering Department
University of Minnesota
Minneapolis, Minnesota 55455

Dr. Keith H. Johnson
Department of Metallurgy and
Materials Science
Massachusetts Institute of Technology
Cambridge, Massachusetts 02139

Dr. S. Sibener
Department of Chemistry
James Franck Institute
5640 Ellis Avenue
Chicago, Illinois 60637

Dr. Arold Green
Quantum Surface Dynamics Branch
Code 3817
Naval Weapons Center
China Lake, California 93555

Dr. A. Wold
Department of Chemistry
Brown University
Providence, Rhode Island 02912

Dr. S. L. Bernasek
Department of Chemistry
Princeton University
Princeton, New Jersey 08544

Dr. P. Lund
Department of Chemistry
Howard University
Washington, D.C. 20059

DL/413/83/01
056/413-2

ABSTRACTS DISTRIBUTION LIST, 056/625/629

Dr. F. Carter
Code 6132
Naval Research Laboratory
Washington, D.C. 20375

Dr. Richard Colton
Code 6112
Naval Research Laboratory
Washington, D.C. 20375

Dr. Dan Pierce
National Bureau of Standards
Optical Physics Division
Washington, D.C. 20234

Dr. R. Stanley Williams
Department of Chemistry
University of California
Los Angeles, California 90024

Dr. R. P. Messmer
Materials Characterization Lab.
General Electric Company
Schenectady, New York 22217

Dr. Robert Gomer
Department of Chemistry
James Franck Institute
5640 Ellis Avenue
Chicago, Illinois 60637

Dr. Ronald Lee
R301
Naval Surface Weapons Center
White Oak
Silver Spring, Maryland 20910

Dr. Paul Schoen
Code 5570
Naval Research Laboratory
Washington, D.C. 20375

Dr. John T. Yates
Department of Chemistry
University of Pittsburgh
Pittsburgh, Pennsylvania 15260

Dr. Richard Greene
Code 5230
Naval Research Laboratory
Washington, D.C. 20375

Dr. L. Kesmodel
Department of Physics
Indiana University
Bloomington, Indiana 47403

Dr. K. C. Janda
California Institute of Technology
Division of Chemistry and Chemical Engineering
Pasadena, California 91125

Dr. E. A. Irene
Department of Chemistry
University of North Carolina
Chapel Hill, Northc Carolina 27514

Dr. Adam Heller
Bell Laboratories
Murray Hill, New Jersey 07974

Dr. Martin Fleischmann
Department of Chemistry
Southampton University
Southampton 509 5NH
Hampshire, England

Dr. John W. Wilkins
Cornell University
Laboratory of Atomic and Solid State Physics
Ithaca, New York 14853

Dr. Richard Smardzewski
Code 6130
Naval Research Laboratory
Washington, D.C. 20375

Dr. H. Tachikawa
Chemistry Department
Jackson State University
Jackson, Mississippi 39217

DL/413/83/01
056/413-2

ABSTRACTS DISTRIBUTION LIST, 056/625/629

Dr. R. G. Wallis
Department of Physics
University of California
Irvine, California 92664

Dr. D. Ramaker
Chemistry Department
George Washington University
Washington, D.C. 20052

Dr. J. C. Hemminger
Chemistry Department
University of California
Irvine, California 92717

Dr. T. F. George
Chemistry Department
University of Rochester
Rochester, New York 14627

Dr. G. Rubloff
IBM
Thomas J. Watson Research Center
P.O. Box 218
Yorktown Heights, New York 10598

Dr. Horia Metiu
Chemistry Department
University of California
Santa Barbara, California 93106

Captain Lee Myers
AFOSR/NC
Bollig AFB
Washington, D.C. 20332

Dr. J. T. Keiser
Department of Chemistry
University of Richmond
Richmond, Virginia 23173

Dr. Roald Hoffmann
Department of Chemistry
Cornell University
Ithaca, New York 14853

Dr. R. W. Plummer
Department of Physics
University of Pennsylvania
Philadelphia, Pennsylvania 19104

Dr. E. Yeager
Department of Chemistry
Case Western Reserve University
Cleveland, Ohio 41106

Dr. N. Winograd
Department of Chemistry
Pennsylvania State University
University Park, Pennsylvania 16802

Dr. G. D. Stein
Mechanical Engineering Department
Northwestern University
Evanston, Illinois 60201

Dr. A. Steckl
Department of Electrical and
Systems Engineering
Rensselaer Polytechnic Institute
Troy, NewYork 12181

Dr. G. H. Morrison
Department of Chemistry
Cornell University
Ithaca, New York 14853

Dr. P. Hansma
Physics Department
University of California
Santa Barbara, California 93106

Dr. J. Baldeschwieler
California Institute of Technology
Division of Chemistry
Pasadena, California 91125

Dr. W. Goddard
California Institute of Technology
Division of Chemistry
Pasadena, California 91125

DL/413/83/01
056/413-2

ABSTRACTS DISTRIBUTION LIST, 056/625/629

Dr. J. E. Jensen
Hughes Research Laboratory
3011 Malibu Canyon Road
Malibu, California 90265

Dr. W. Knauer
Hughes Research Laboratory
3011 Malibu Canyon Road
Malibu, California 90265

Dr. J. H. Weaver
Department of Chemical Engineering
and Materials Science
University of Minnesota
Minneapolis, Minnesota 55455

Dr. C. B. Harris
Department of Chemistry
University of California
Berkeley, California 94720

EN

FILME

12-84

DTIC